drones

MDPI

Article

Temporal Monitoring of Simulated Burials in an Arid Environment Using RGB/Multispectral Sensor Unmanned Aerial Vehicles

Abdullah Alawadhi [1], Constantine Eliopoulos [1,*] and Frederic Bezombes [2]

[1] Faculty of Science, Liverpool John Moores University, Liverpool L3 3AF, UK; alawadhias@gmail.com
[2] Faculty of Engineering and Technology, Liverpool John Moores University, Liverpool L3 3AF, UK; f.bezombes@ljmu.ac.uk
* Correspondence: c.eliopoulos@ljmu.ac.uk

Abstract: For the first time, RGB and multispectral sensors deployed on UAVs were used to facilitate grave detection in a desert location. The research sought to monitor surface anomalies caused by burials using manual and enhanced detection methods, which was possible up to 18 months. Near-IR (NIR) and Red-Edge bands were the most suitable for manual detection, with a 69% and 31% success rate, respectively. Meanwhile, the enhanced method results varied depending on the sensor. The standard Reed–Xiaoli Detector (RXD) algorithm and Uniform Target Detector (UTD) algorithm were the most suitable for RGB data, with 56% and 43% detection rates, respectively. For the multispectral data, the percentages varied between the algorithms with a hybrid of the RXD and UTD algorithms yielding a 56% detection rate, the UTD algorithm 31%, and the RXD algorithm 13%. Moreover, the research explored identifying grave mounds using the normalized digital surface model (nDSM) and evaluated using the normalized difference vegetation index (NDVI) in grave detection. nDSM successfully located grave mounds at heights as low as 1 cm. A noticeable difference in NDVI values was observed between the graves and their surroundings, regardless of the extreme weather conditions. The results support the potential of using RGB and multispectral sensors mounted on UAVs for detecting burial sites in an arid environment.

Keywords: remote sensing; grave detection; drone; multispectral; MSI; forensic; photogrammetry; NDVI

Citation: Alawadhi, A.; Eliopoulos, C.; Bezombes, F. Temporal Monitoring of Simulated Burials in an Arid Environment Using RGB/Multispectral Sensor Unmanned Aerial Vehicles. *Drones* **2024**, *8*, 444. https://doi.org/10.3390/drones8090444

Academic Editor: Giordano Teza

Received: 11 July 2024
Revised: 21 August 2024
Accepted: 24 August 2024
Published: 29 August 2024

1. Introduction

Around the world, many populations have suffered from human rights violations throughout history. A recent example is the Ukrainian and Russian war, where reports described a wide range of violations of human rights from both sides, including war crimes and unmarked clandestine mass graves [1]. A forensic investigation plays a significant role in mass grave detection and exhumation to help provide closure for surviving families and prove the occurrence of a human rights violation [2]. Current practice suggests a phased approach in detecting burials in which the search moves from large-scale (macro-scale) remote sensing methods to the application of medium-range geophysical technology, and finally, a ground search (micro-scale) for a specific and defined area of interest [3]. One of the early uses of remote sensing in detecting and identifying burial sites was during the investigations of the International Criminal Tribunal for the former Yugoslavia (ICTY), when aerial and satellite images from the US government helped search for clandestine graves [2]. The aim of this research was to help narrow down the search area of a burial site using a remote sensing approach. More specifically, the captured images using remote sensing techniques were used to interpret surface anomalies that might indicate a suspected burial site. For optimal results, combining different remote sensing techniques improves the success rate in detecting and identifying clandestine graves. However, each scenario is

case-specific, and the techniques that might show a success rate of identification in one case might not be helpful in another due to various reasons, such as differences in the vegetation cover and terrain features [4].

Past research has demonstrated that remote sensing can detect burial sites in various environments using techniques such as hyperspectral imaging (HSI), light detection and ranging (LiDAR), multispectral imaging (MSI), true color RGB, and thermal imaging (TI) [2,5–11]. However, in arid environments, only the costly HSI and TI have been used to detect buried remains [12,13]. HSI successfully detected the graves for almost six months post-burial, and the useful wavelength intervals were mainly distributed along the spectral range of 700–1800 nm [12]. While in a TI analysis, it was possible to detect clandestine graves in an arid environment by distinguishing heat and soil moisture differences between the graves and their surroundings. The former was successful in detecting graves for seven months, while the latter was successful for ten months [13]. The impetus for the present study was the need to have accessible imaging techniques that could help arid countries with limited resources detect graves following armed conflicts. Hence, the research presented here aimed to explore the effectiveness of using RGB and multispectral sensors deployed on unmanned aerial vehicles (UAVs) in temporally monitoring and detecting soil disturbances, differences in ground elevation level and differences in normalized difference vegetation index (NDVI) values in an arid environment, with the purpose of helping to locate clandestine graves.

2. Materials and Methods

2.1. Study Area

The research took place in Kuwait, a country bordering Iraq to the north and the Kingdom of Saudi Arabia to the south. Situated within the desert geographic zone in the Middle East, Kuwait experiences a continental environment marked by its lengthy summers and brief, mild winters, occasionally accompanied by rainfall. Temperatures can sometimes reach 50 °C in the shade, and dust storms are a common occurrence during the summer months. Despite its brevity, the winter in Kuwait remains relatively warm, although temperatures can occasionally drop to 0 °C in the desert. The autumn and spring seasons are notable for their short durations [14]. A permit was obtained from the Environment Public Authority in Kuwait to construct the research area in a remote, dry, flat, non-vegetated 900 m^2 plot in a Nature Reserve that is not accessible by the public and located in the north Kuwaiti desert (29.3621° N, 47.6931° E), which was fenced and secured to avoid any human intrusion to the site. The site consisted of dry, rough, uniform soil with no vegetation cover. The site was chosen to be consistent with the harsh and arid environment that was encountered previously at burial sites in the region [15,16].

Ten freshly slaughtered and skinned sheep were purchased from a local slaughterhouse. The internal organs of the sheep were kept intact, and each sheep was separately wrapped in a plastic bag and transferred to the research area to get buried. Pigs have always been the first choice as an analogue to humans when conducting a forensic experiment as they possess similar chemical composition, size, tissue-to-body fat ratios, and skin/hair type to humans [17]. However, pigs are not available in Kuwait due to religious reasons. Alternatively, sheep were the closest equivalent available to use for the experiment, and it is not the first time mammals other than pigs have been used in such an experiment [18]. The sheep used in this research were procured from a local abattoir and had an average weight of 32 kg, falling within the recommended carcass weight range (22 to 35 kg) for experimental research involving a human analogue, which also aligns with the average weight of an adult human torso [19]. The utilization of animals in this study adhered to the ethical guidelines established by Liverpool John Moores University for conducting research involving animals, which prohibit carrying out investigations on living vertebrates that might cause pain, suffering, distress, or lasting harm.

A total of six graves were simulated for the purpose of the present research. All graves were at least 5 m apart to avoid cross-contamination or interference from the decomposition

fluids of the buried animals [20]. The graves were excavated and backfilled either by a hand tool (shovel) or using a machine (Caterpillar backhoe loader with a bucket size of 60 cm and loader size of 240 cm). Three out of the six graves served as control graves with no buried sheep in them, simulating soil disturbance caused by factors other than being a burial site, such as digging related to construction. The first control grave was a single shallow (50–60 cm) hand-dug grave (G1), the second one was a single deep (100–150 cm) grave dug with a backhoe (G3), and the last one was a deep (150 cm) mass grave (G5) dug with a backhoe. On the other hand, with the same relevant depth as the control graves, the first experimental grave was a hand-dug shallow grave with a single sheep (G2). The second experimental grave was a deep grave dug with a backhoe (G4), also with a single sheep. The last experimental grave was a mass grave occupied by eight sheep (G6). Clothes, placed on top of the sheep, and 9 mm handgun shell cases, placed around the sheep, were added to the experimental graves to make them resemble a real-life scenario. Table 1 illustrates a summary of grave-related information.

Table 1. Summary of grave-related information.

Grave	Single/Mass Grave	Method of Digging	Depth (cm)	Grave Content	Control/ Experimental
G1	Single	Hand dug	30	N/A	Control
G2	Single	Hand dug	40	1 sheep 2 shell cases 1 cotton sweater	Experimental
G3	Single	Machine dug	60	N/A	Control
G4	Single	Machine dug	80	1 sheep 2 shell cases 1 cotton pants	Experimental
G5	Mass	Machine dug	150	N/A	Control
G6	Mass	Machine dug	150	8 sheep 2 shell cases 1 denim jeans 2 cotton grey socks 1 cotton black dress 1 cotton white underwear	Experimental

Figure 1 shows unmodified aerial images of the research area using RGB and NIR wavelength bands taken one week post-burial.

2.2. UAV Image Acquisition

Permission was obtained from the Ministry of Interior in Kuwait to fly the UAVs, which was restricted only to the allocated research area due to its proximity to an airbase. Two types of multi-rotor UAVs coupled with different imaging sensors were used to capture 18 sets of images using the Pix4Dcapture software [21]. The visible light (RGB) sensor was used to capture 18 sets of images for the entire research period, which lasted for 18 months. On the other hand, the multispectral imaging (MSI) sensor captured the same number of images as the RGB except for the last month, due to a technical issue with the UAV. The UAVs were flown at an altitude of 30 m, which yielded a ground sampling distance (GSD) that laid within the recommended 10 cm/pixel for both sensors used [22].

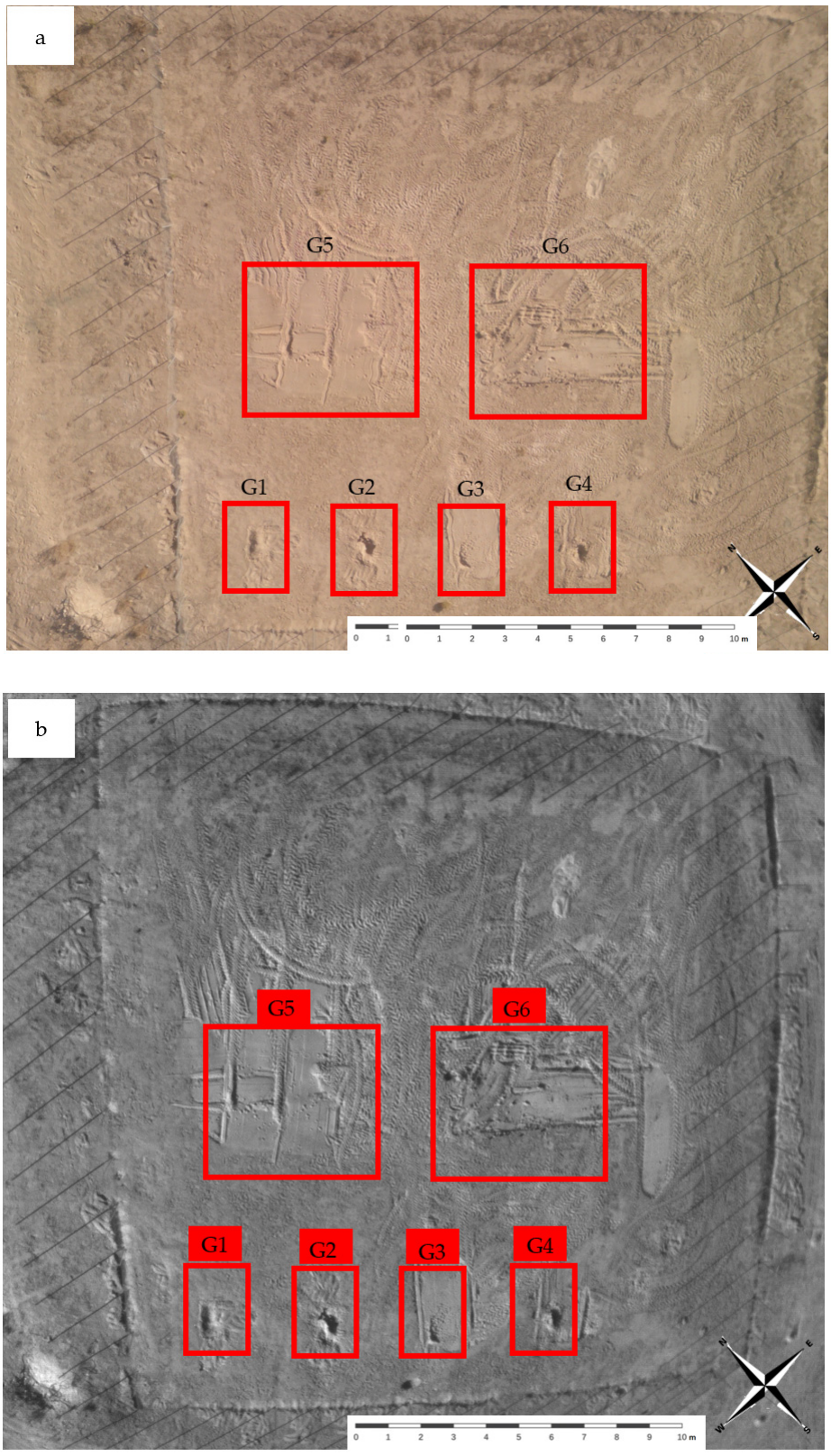

Figure 1. Aerial images of the research area using (**a**) RGB and (**b**) NIR wavelength bands, one week post-burial. G1–G6: Grave 1–Grave 6.

2.3. UAV Platforms and Sensors

A Parrot Anafi UAV equipped with a 21 MP SONY IMX230 1/2.4″ sensor (Sony, Tokyo, Japan) was used to capture the RGB images [23]. On the other hand, a Parrot

Bluegrass (Parrot Bluegrass, Paris, France) was used for the MSI image acquisition. It comes with a preinstalled front 16-megapixel RGB camera, which shoots both still and video in full HD (1080 p). It is also equipped with a Parrot Sequoia multispectral sensor, which captures images in RGB with a resolution of 4608 × 3456 and captures Green, Red, Red-Edge, and Near-Infrared (NIR) wavelength bands with a 1280 × 960 resolution. It also comes with a fully integrated sunshine sensor that captures and logs the lightning conditions for calibration purposes to ensure the digital number (DN) obtained is an accurate representation of the captured images on the day [24].

2.4. Image Processing

Upon linking the UAVs to the photogrammetry software Pix4Dcapture [21], the UAV and its attached sensor were calibrated by following the provided guidelines in the software. Following that, the flight was planned, and the images were set to be captured using the software. Once the images were captured, and the flight mission was over, the captured images were then transferred to the photogrammetry software Pix4Dmapper for the initial processing phase and some feature extraction for the research area [21]. Each time the images were captured, the RGB images were used to extract a digital terrain model (DTM), digital surface model (DSM), and an orthomosaic map of the area using the Pix4Dmapper. An orthomosaic map is an image with great detail and resolution (it can reach as low as 1 cm/pixel depending on the various aspects such as UAV height and sensor used) made by combining overlapping images to construct drone-based reflectance maps of an area of interest [25]. A reflectance map is an orthomosaic monochromatic image used to calculate vegetation indices such as the NDVI, where each pixel on it is radiometrically calibrated, contains surface reflectance values ranging from 0 to 1, and shows a different amount of light and similar hue in a specific spectral band [26]. On the other hand, depending on the type and source of the digital elevation model (DEM), the elevation values describe the ground surface excluding all objects above, which is known as the DTM, or it represents the actual surface including all objects rising above the terrain, which is known as the DSM [27]. Therefore, subtracting the DTM from DSM results in a normalized digital surface model (nDSM), which is a representation of objects rising from the terrain, and in our case, the grave mounds.

Meanwhile, MSI was used to extract the normalized difference vegetation index (NDVI) map and multiple orthomosaics of the area (Red, Red-Edge, and NIR). An additional step in processing the MSI images with Pix4Dmapper was to calibrate the images using an image captured from a calibration target, right before or after the flight, to match the weather and lighting conditions to the ones during the flight [26].

Once the images were captured and processed, the extracted DTMs, DSMs, and orthomosaics were exported to image and geospatial analysis and processing software for further analysis. The multiple-band RGB orthomosaics were exported to ENVI by L3HARRIS (V2.3.1), an image processing and analysis software, to detect surface anomalies both manually and using an enhancement tool. The manual method was conducted by macroscopically visualizing any anomalies in the extracted orthomosaic using Windows Photos software (2019.19071.12548.0) that might indicate the location of the grave without using any enhancement methods, coloring tools, or specialized computer software. It included targeting surface features such as soil disturbance and differences in vegetation distribution. Alternatively, the enhanced method of detection was conducted using the RX Anomaly Detection tool available in ENVI [28]. It is an enhancement tool that implements the workflow of the Reed–Xiaoli Detector (RXD) algorithm, which extracts targets that are spectrally distinct from the image background and identify them as anomalies in a multiband image, an algorithm developed by Reed and Yu [29]. Three anomaly detection methods are available to choose from in the ENVI RX Anomaly Detection tool based on the chosen algorithm: RXD, Uniform Target Detector (UTD), and a hybrid of the RXD and UTD methods (RXD-UTD) [29,30]. On the other hand, the extracted DTMs and DSMs were exported to the Esri ArcMap application (10.8.2), a geospatial processing software designed

by ArcGIS Desktop, to calculate the nDSMs of the research area using the Map Algebra tool—Raster Calculator feature [31]. This nDSM of the enclosed research area was used to identify surface outliers related to grave mounds. Moreover, the RGB orthomosaics were visualized for manual inspection for any surface anomalies caused by the graves without using any enhancement tools.

Similarly to the RGB images, the single-band MS orthomosaics were exported to ENVI v.5.6 by L3HARRIS to combine them into a multiple-band orthomosaic image using the Layer Stacking tool [32]. Then, the stacked image was processed using the Anomaly Detection tool in ENVI to detect surface anomalies with an enhancement tool. In addition, the Esri ArcMap application was used to preview and manually detect surface anomalies of the single-band MS orthomosaics by visualizing the image and looking for the outplaced pixels in the image.

3. Results

3.1. RGB Imaging

The nDSM successfully distinguished surface elevation differences between the graves and their surroundings. The method was successful in detecting height differences as low as 1 cm. An average of the obtained nDSM values from the surfaces of the graves was calculated, which indicated the height of the graves. The results showed a sharp elevation loss in the experimental graves the first three days post-burial due to scavenger intrusion and their attempt to dig out the buried sheep. Afterwards, all graves showed a steady trend of elevation loss. Table 2 illustrates the height of grave mounds measured on-ground, using a measuring tape placed on the center of the grave and flattened against the ground surface, and the height of the graves, calculated from the DTM and DSM layers throughout the experiment.

Figure 2 illustrates the nDSM map calculated two months post-burial.

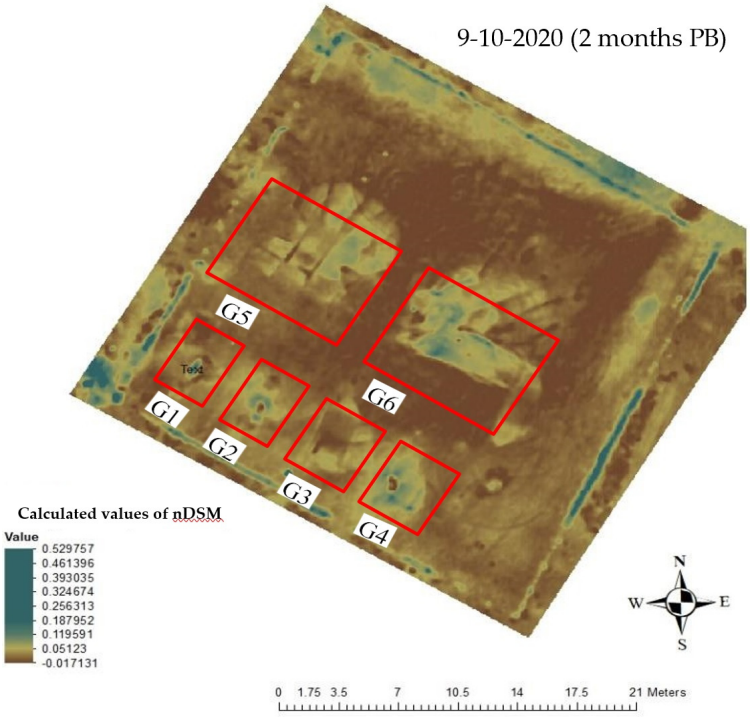

Figure 2. The nDSM map of the research area calculated two months post-burial. G1–G6: Grave 1–Grave 6.

Table 2. Grave height measurement obtained from the nDSM and their relevant on-ground measurement in centimeters. nDSM: digital elevation model, PB: post-burial.

Day Measured	Height Measured	Grave 1	Grave 2	Grave 3	Grave 4	Grave 5	Grave 6
Day of digging	On-ground	12	12.5	3	0	6	17
	nDSM	12.6	13.7	3.9	2.5	7.9	13.9
1 day PB	On-ground	12	6	0	0	6	7
	nDSM	11.9	7	1	2.5	7	7
3 days PB	On-ground	10.8	−8	0	−9	6	5
	nDSM	11.5	1	1	0	7	7
1 week PB	On-ground	8	−10	0	−9	4	5
	nDSM	11	3	0	0	3.6	8.3
2 weeks PB	On-ground	8	−10	0	−11	4	5
	nDSM	10	3	1	1	1	8.4
3 weeks PB	On-ground	8	−8	0	−10.5	4	4
	nDSM	10	1	1	1	3	7
1 month PB	On-ground	8	−10	0	−11	4	4
	nDSM	11	0.7	2.7	1	2.7	6.4
2 months PB	On-ground	8	−10	−1	−12	4	3
	nDSM	10	0.7	1.7	0.6	8	6.5
3 months PB	On-ground	7	−10	−2	−12	3	3
	nDSM	9.3	1.1	1.6	0.3	4	5.7
6 months PB	On-ground	5.5	−6	−5.5	−10	0	4
	nDSM	7.9	1.2	1.2	0.2	1.2	5.9
7 months PB	On-ground	5.5	−6	−6	−8	0	3.2
	nDSM	7.6	1.5	3.5	0.5	3.5	5.2
9 months PB	On-ground	5	−3	−5.5	−9	0	3
	nDSM	7.2	1.5	3.5	0.5	2.2	4.1
10 months PB	On-ground	3	−2	−2.5	−5.5	0	2
	nDSM	4.2	1.3	1.3	0.3	3.6	4.2
11 months PB	On-ground	3	−1.5	−2	−4.5	0	2
	nDSM	2.8	1.3	1.3	1.3	2.7	3.5
12 months PB	On-ground	2.5	−1.5	−1.5	−4.5	0	2
	nDSM	2	1.8	1.8	1.2	2.4	3.2
15 months PB	On-ground	2	−1	−1	−2	0	1
	nDSM	2.6	1.2	1.2	1.2	1.4	2.5
18 months PB	On-ground	1	−1	−1	−1	0	1
	nDSM	2.7	1.3	1.3	1.3	1.6	2.1

The manual method was successful for 15 months post-burial for all graves, except G4, which was visible until the ninth month only and then again at 15 months. It was successful in finding which surface anomalies on the graves were detectable and could be clearly identified when the area was macroscopically visualized. The images captured in the eighteenth month did not show any type of soil disturbances or indications that could be used to locate the graves. On the other hand, the automated method proved to be successful during the entire period of the experiment, with RXD and UTD being the most suitable methods of detection. Out of the 16 times when the images were analyzed, the RXD algorithm performed better on nine occasions (56%), while the UTD algorithm was favorable in the remaining times (44%). Table 3 lists the most appropriate method of detection used throughout the experiment.

Table 3. The best method of detection when applying the RX Anomaly Detection Tool on RGB images. PB: post-burial.

Collection Date	Method of Detection	G1	G2	G3	G4	G5	G6
1 day PB	RXD	✓	✓	✓	✓	✓	✓
3 days PB	RXD	✓	✓	✓	✓	✓	✓
7 days PB	RXD	✓	✓	✓	✓	✓	✓
14 days PB	RXD	✓	✓	✓	✓	✓	✓
21 days PB	RXD	✓	✓	✓	✓	✓	✓
1 month PB	RXD	✓	✓	✓	✓	✓	✓
2 months PB	RXD	✓	✓	✓	✓	✓	✓
3 months PB	UTD	✓	✓		✓	✓	✓
6 months PB	UTD	✓		✓		✓	✓
7 months PB	UTD	✓	✓	✓	✓	✓	✓
9 months PB	UTD			✓		✓	✓
10 months PB	UTD	✓	✓	✓	✓	✓	✓
11 months PB	UTD	✓	✓	✓	✓	✓	✓
12 months PB	UTD	✓	✓	✓	✓	✓	✓
15 months PB	RXD	✓			✓	✓	✓
18 months PB	RXD	✓	✓	✓	✓	✓	✓

Figure 3 illustrates the difference between the manual and enhanced method of detection of the research 15 months post-burial.

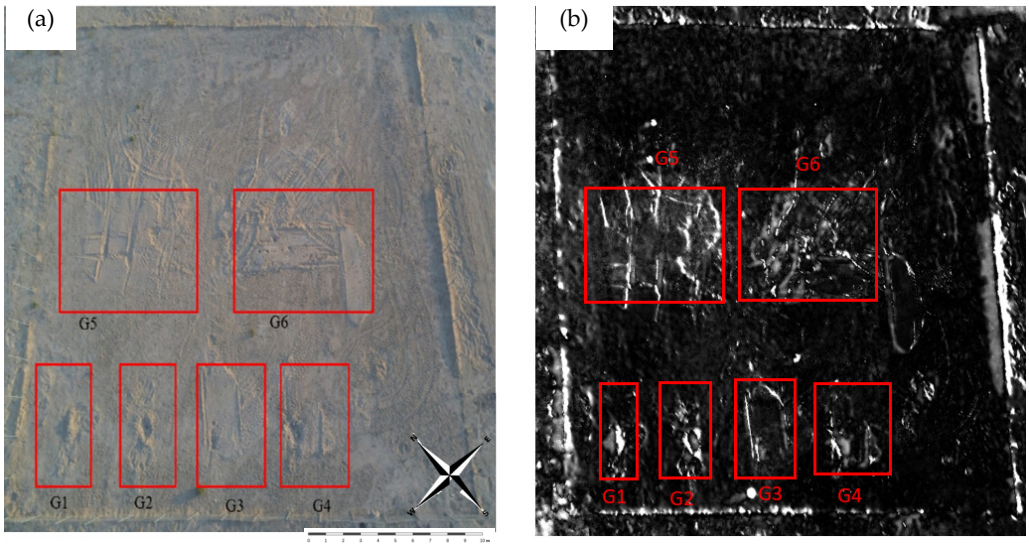

Figure 3. The (**a**) manual and (**b**) enhanced anomaly detection methods 15 months post-burial using an RGB sensor. G1–G6: Grave1–Grave6.

3.2. Multispectral Imaging

Unlike the regular RGB sensor, which is limited to three wavelength bands, MSI records a broad range of spectral bands from visible light to Near-Infrared (NIR) wavelength bands. Hence, when combined with witness testimony, MSI can be very useful in searching for a suspected area that might contain a burial site. Therefore, MSI is considered to be a beneficial spectral imaging sensor to expose surface anomalies using different light reflectance sources invisible to the human eye. A previous study used MSI to identify burial mounds and subsurface remains that represented permanent settlements built from durable materials in Bulgaria and Italy [33]. In the present study, the image analysis was used to evaluate and temporally monitor the use of multispectral imaging in detecting surface anomalies that could indicate the presence of a clandestine grave both manually and using enhancement tools and the usefulness of using the NDVI in the process. The manual method results revealed that the NIR and Red-Edge wavelengths had the most

details that could aid this process. The NIR output had the best band to visualize the surface anomalies in 11 of the 16 data sets collected, while the Red-Edge was the best detection method for the other 5 data sets, in which the NIR band was the second-best (NIR, 69% and Red-Edge, 31%). Meanwhile, throughout the research, the Green band had the lowest detection rate among all the spectral bands, showing the least amount of information on the images. Table 4 indicates the arrangement level of the bands most suitable for each data collection date and the identified MSI wavelength bands most suitable for each data collection date.

Table 4. MSI wavelength bands most suitable for each data collection date. PB: Post-burial.

Collection Date	Bands Detection Level			
	High			Low
1 day PB	Red-Edge	NIR	Red	Green
3 days PB	Red-Edge	NIR	Red	Green
7 days PB	Red-Edge	NIR	Red	Green
14 days PB	NIR	Red	Red-Edge	Green
21 days PB	NIR	Red-Edge	Red	Green
1 month PB	NIR	Red	Red-Edge	Green
2 months PB	NIR	Red	Red-Edge	Green
3 months PB	NIR	Red	Red-Edge	Green
6 months PB	NIR	Red-Edge	Red	Green
7 months PB	NIR	Red-Edge	Red	Green
9 months PB	NIR	Red-Edge	Red	Green
10 months PB	Red-Edge	NIR	Red	Green
11 months PB	NIR	Red-Edge	Red	Green
12 months PB	Red-Edge	NIR	Red	Green
15 months PB	NIR	Red-Edge	Red	Green
18 months PB	NIR	Red-Edge	Red	Green

In addition, the enhanced method of detection that ran on the MSI using the RX Anomaly Detection Tool in ENVI proved successful for almost the entire period of the experiment. It was able to successfully detect surface anomalies in all graves in 10 out of 15 data sets captured. In the other five data sets, the anomaly detection method successfully detected between four and five surface anomalies on the graves. The tenth-month post-burial analysis could not detect surface anomalies related to the graves. The best outcomes for the multispectral sensor method were obtained using a hybrid of the RXD and UTD algorithms (RXD-UTD) (56.25%), UTD (31.25%), and RXD (12.5%). Table 5 illustrates the method of detection used and which graves were detectable when the RX Anomaly Detection tool was used on the MSI data.

Figure 4 illustrates the application of the RXD-UTD anomaly detection method twelve months post-burial.

The NDVI is a graphical indicator mainly used in agriculture, biology and other geosciences to measure healthy vegetation [34]. However, here, the NDVI index was applied as an explanatory contribution in bare-soil moisture estimation, similar to experimental conditions previously conducted, since the research was carried out in a desert environment lacking vegetation cover [35]. It is calculated using the Near-Infrared (NIR) and Red spectral bands, and its values always lie between -1 and 1. The closer the number is to one, the higher the indication that the soil is moist.

$$\mathrm{NDVI} = \frac{\mathrm{NIR} - \mathrm{Red}}{\mathrm{NIR} + \mathrm{Red}} \quad (1)$$

where NIR is the calibrated wavelength value of the Near-Infrared spectral band, and Red is the calibrated wavelength value of the Red spectral band captured from an MSI camera.

Table 5. The graves which were detected when applying the RX Anomaly Detection Tool on MSI data. PB: post-burial.

Collection Date	Method of Detection	G1	G2	G3	G4	G5	G6
1 day PB	UTD	✓	✓	✓	✓	✓	✓
3 days PB	UTD	✓	✓	✓	✓	✓	✓
7 days PB	UTD	✓	✓	✓	✓	✓	✓
14 days PB	RXD-UTD	✓	✓	✓	✓	✓	✓
21 days PB	RXD-UTD	✓	✓	✓	✓	✓	✓
1 month PB	RXD-UTD	✓	✓	✓	✓	✓	✓
2 months PB	RXD-UTD	✓	✓	✓		✓	✓
3 months PB	RXD-UTD	✓	✓			✓	
6 months PB	RXD	✓	✓	✓	✓	✓	✓
7 months PB	RXD	✓	✓	✓	✓	✓	✓
9 months PB	RXD-UTD	✓	✓	✓	✓		✓
10 months PB	UTD						
11 months PB	RXD-UTD	✓	✓	✓	✓	✓	
12 months PB	RXD-UTD	✓	✓	✓	✓	✓	✓
15 months PB	UTD		✓		✓	✓	✓

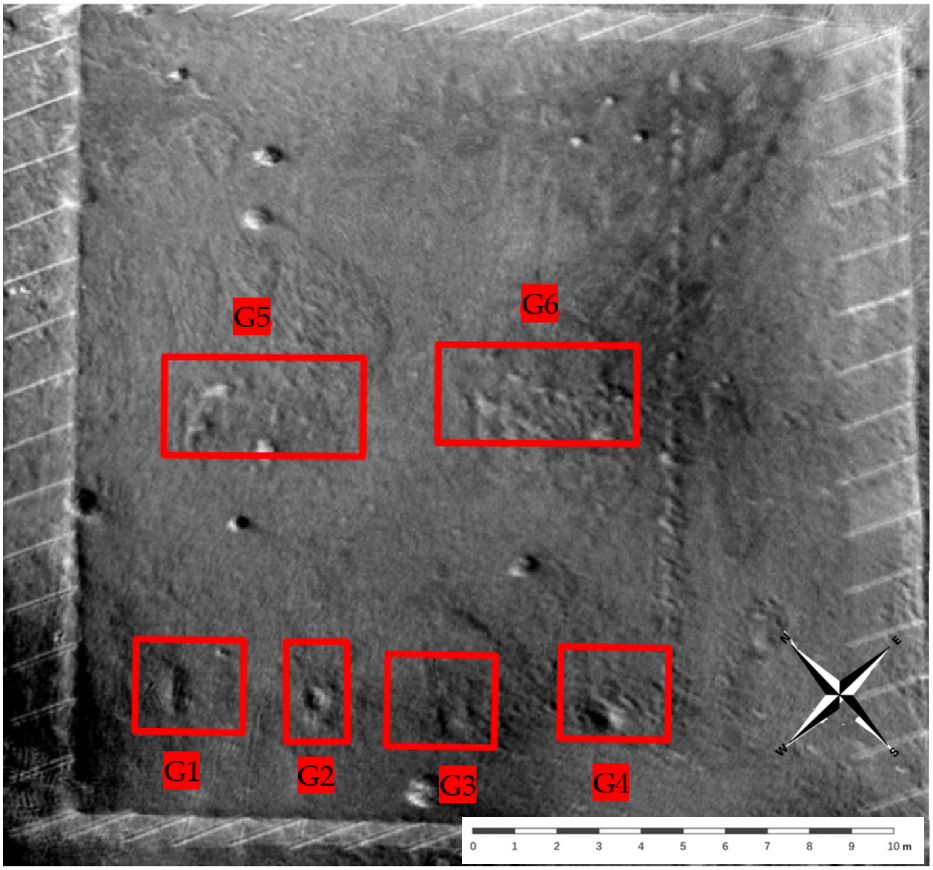

Figure 4. The application of the RXD-UTD anomaly detection method on the MSI image, twelve months post-burial. G1–G6: Grave 1–Grave 6.

MSI was used to explore and temporally monitor whether variations in NDVI over time could help detect the location of a grave in an arid environment lacking dense vegetation. Generally, the graves had modest differences in NDVI values compared to their surroundings, except for the seventh month post-burial, where the experimental mass grave (G6) showed a considerably high difference (0.33) compared to its surroundings (Figure 5). Therefore, when examining the obtained results, graves were mainly categorized under the "open soil and sparse vegetation classes" [36]. Table 6 illustrates the obtained

NDVI values of the graves throughout the 18-month research period, along with the highest and lowest NDVI values recorded for the surroundings.

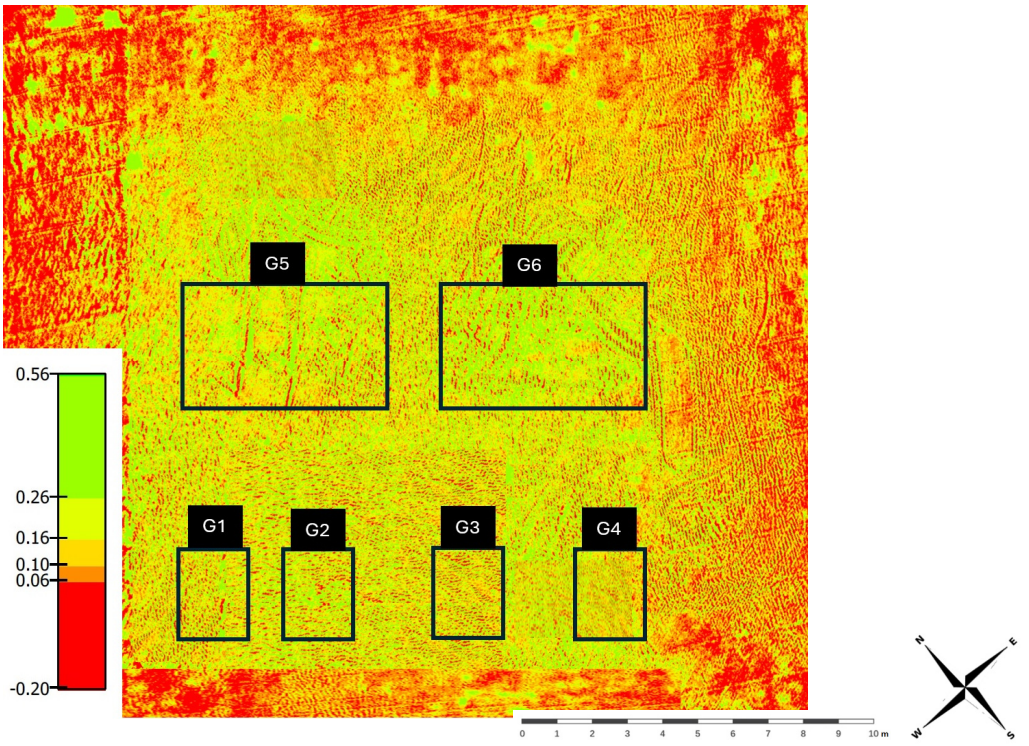

Figure 5. The NDVI map of the surveyed area, seven months post-burial. G1–G6: Grave 1–Grave 6.

Table 6. NDVI values for both graves throughout the research period, along with the highest and lowest NDVI values of the surrounding area. PB: post-burial.

Collection Date	Highest Value	Lowest Value	G1	G2	G3	G4	G5	G6
3 days PB	0.19	0.03	0.04	0.04	0.08	0.07	0.1	0.15
7 days PB	0.17	0.03	0.04	0.04	0.09	0.08	0.15	0.16
14 days PB	0.12	0.02	0.03	0.04	0.07	0.09	0.15	0.17
21 days PB	0.12	0.02	0.02	0.02	0.03	0.04	0.09	0.12
1 month PB	0.14	0.04	0.02	0.02	0.03	0.04	0.1	0.13
2 months PB	0.2	0.06	0.06	0.07	0.07	0.08	0.19	0.2
3 months PB	0.17	0.06	0.07	0.07	0.09	0.08	0.16	0.17
6 months PB	0.49	0.2	0.25	0.27	0.31	0.32	0.42	0.48
7 months PB	0.56	0.3	0.23	0.24	0.29	0.31	0.4	0.56
9 months PB	0.43	0.2	0.2	0.2	0.25	0.27	0.38	0.42
10 months PB	0.35	0.12	0.14	0.13	0.2	0.22	0.31	0.34
11 months PB	0.32	0.08	0.09	0.08	0.19	0.21	0.25	0.3
12 months PB	0.21	0.05	0.07	0.08	0.12	0.14	0.21	0.21
15 months PB	0.18	0.04	0.06	0.06	0.09	0.07	0.15	0.16
18 months PB	0.35	0.07	0.07	0.07	0.09	0.08	0.17	0.18

Figure 5 illustrates the NDVI map of the surveyed area seven months post-burial.

4. Discussion

The research presented here aimed to temporally monitor and evaluate a cost-effective detection method when searching for clandestine graves in an arid environment. RGB image analysis results sought to help detect surface anomalies and measure the digital elevation model of the enclosed research area. A multispectral image analysis evaluated the use of multispectral imaging in detecting surface anomalies that could indicate the presence of a clandestine grave and the usefulness of using the NDVI in the process. In 2002, a revolutionary search method was introduced to the field of forensic science in which multispectral data with a resolution of 15 m/pixel from the ASTER satellite were used to detect a mass grave in Guatemala during a retrospective study [4]. Since then, using multispectral imaging to locate clandestine burials has been a well-documented area within forensic science and suggested as a helpful technique in various environments [4,37–42]. However, it has not been utilized in an arid environment before.

4.1. RGB Sensor

4.1.1. nDSM

An unmodified RGB digital camera deployed on a UAV has proved its effectiveness in detecting clandestine burials on numerous occasions [2,8,41,43,44]. It might be argued that capturing those images in such narrow spectral bands limits the use of this sensor in grave detection methods. However, when using the appropriate software and applying the proper tools to the captured images, the results might become substantial in aiding the detection process. Areas that are non-vegetated and have open landscapes with no ground obstacles, similar to the presented research area, are preferable when looking for clandestine graves when using aerial sensors [41]. For the present research, the captured RGB images were processed with multiple software tools to analyze the findings and investigate their effectiveness in identifying any surface elevation in the enclosed area that can resemble an outlier using the nDSM technique. Furthermore, RGB images were analyzed to explore their usefulness in detecting surface anomalies caused by digging and refilling the graves.

Akin to the previously published literature where the digital terrain model (DTM) and digital surface model (DSM) were used and successfully demonstrated the effectiveness of such features in detecting clandestine graves [4,42,45], the present research findings collectively support using such features to detect clandestine graves. The calculated nDSM values listed in Table 4 illustrate that this feature could be used to detect surface elevation in an arid environment for up to 18 months in our research conditions. Another study conducted explored the effectiveness of using terrestrial Light Detection and Ranging (LiDAR), which is far more complex and precise, in identifying elevation changes associated with unmarked graves [11]. It found that a decrease in elevation was detected immediately after the creation of the burial and persisted for up to 108 days. Thus, the research findings using the affordable technology presented in that study showed good results, which could be used in the detection method for burial mounds while they still exist.

4.1.2. Anomaly Detection

The anomaly detection on the RGB images was investigated manually and using an enhancement tool. Upon checking, the orthomosaic maps of the research area had a clear image of soil disturbance for all graves for the first three months. This clarity was expected since the area was isolated from human and mechanical intrusions and only exposed to nature and its wildlife. In addition, the first three months remained out of the rainy season of the country. Hence, this manual detection of soil disturbance was more likely to be possible for the first three months. As far as the sixth- and seventh-month data are concerned, where only G5 and G6 were detectable, the vegetation growth of the area played a major factor in obstructing the soil disturbance that appeared on the other graves, and the graves were less detectable and defined. Toward the tenth month, graves G1, G2, G3, and G4 became visible again; this can be related to the fact that the vegetation cover of the research area dried out, and the topsoil of the graves got more defined and shaped

from the rainwater absorption. This detection was possible until the fifteenth month but not for the last set of data collected in the eighteenth month.

Alternatively, the obtained results from the automated soil disturbance detection method on the RGB images demonstrated encouraging technology usage in such arid conditions. Until the second month post-burial, RXD was the best detector to distinguish soil disturbance automatically. While RXD extracts targets that are spectrally distinct from the image background, UTD extracts background signatures as anomalies and provides a reasonable estimate of the image background. Hence, referring to Table 3, RXD was a more suitable detector than UTD for the first two months since the area did not undergo any changes in environmental or climatic conditions except for the disturbance caused by the digging and backfilling of the graves. However, the situation was different when capturing data from the third month and toward the twelfth month. There was a seasonal weather change, and the area experienced rainy days and vegetation growth. Hence, topsoil disturbances became more detailed after absorbing the rainwater. Ultimately, the background signatures were extracted as anomalies and a good estimate of the image background was provided. Therefore, the UTD detector was more applicable in this period. Afterwards, with the twelfth- and fifteenth-month post-burial data, and after the area had completely dried out, the RXD detector was once again a more effective detector to be used with the obtained images. Out of the 18 sets of images collected and examined, the detectors could not identify all graves on 4 occasions. In the first, third, and sixth months of post-burial data, the detectors could identify five out of the six graves. Moreover, the detectors could identify three out of six graves in the ninth and fifteenth months post-burial. However, none of the non-detected graves was a mass grave on all those undetectable occasions. Consequently, it can be inferred that the technique works better with larger graves than smaller ones since more disturbance can be detected.

4.2. MSI Sensor

4.2.1. Anomaly Detection

Similarly to RGB imaging, detecting surface anomalies in multispectral imaging was carried out manually and using enhancement tools. The results were successful until the last set of data collected for the multispectral imaging, which was 15 months post-burial. When manually viewing those images captured at those wavelengths and trying to identify any surface anomalies in the images, NIR and Red-Edge represented the optimal spectral regions for anomaly detection. The detectability of the NIR wavelength band was consistent with the reported results from the previously published literature where multispectral and hyperspectral imaging techniques were used to detect anomalies caused by potential burial sites [12,38,44,46,47]. Moreover, the findings of other studies revealed that imaging techniques readily distinguished the graves from soil disturbances for 16 months using the reflectance spectra [2,5]. Likewise, the present results also demonstrated the capability of the multispectral imaging technique to distinguish such disturbance for a similar period.

Unlike the obtained high-resolution RGB images, MS images were less detailed and had less image resolution. Furthermore, the research area was in an arid environment, and anomalies were not easily distinguished. Moreover, RXD-UTD suppresses the background and enhances anomalies and is most suitable when the anomalies have an energy level equal to or less than the background [30]. Hence, it was expected that the most suitable detection method for this type of imaging would be RXD-UTD when analyzing the images automatically using the RX Anomaly Detection Tool in ENVI. However, the exception of the tenth month post-burial, which failed to capture any anomaly on all graves, remains unjustifiable since the disturbance was visible upon examining the images manually.

4.2.2. NDVI

When the present research is compared to the existing published literature regarding the use of the NDVI to measure vegetation health to help locate clandestine graves, it is essential to note that it is not directly comparable. The main reason is that the research

environment and the vegetation coverage do not resemble what has been previously studied. When comparing the graves to their surroundings, there was a slight variation between the NDVI values. The research environment is considered one of the hottest in the world, and vegetation growth is not very common in such an arid environment due to the dryness of the ground and lack of rain and nearby natural water resources. In addition, the burial was classified as a deep grave (carcasses were buried at 1.5 m). At this depth, the decomposition process and the release of nutrients might take years, depending on interrelated environmental variables such as soil pH, humidity, temperature, and others [48]. Hence, only a minor difference in NDVI between the graves and the adjacent surroundings was noticed.

4.3. Limitations

Also, it is acknowledged that one limitation of the current research is the restrictions of airspace regulations due to the proximity of the research area location to an airbase. In addition, flying permission was obtained from the Ministry of Interior in Kuwait to operate the UAV, which forbids the capturing of any images outside the research area. This limited us from testing the technology used for false positives and false negatives, which would have provided us with more information on the utility of commercially available UAVs in aiding clandestine grave detection methods. Another limitation is that alterations in different soil and vegetation patterns were not heavily studied nor observed in much detail. A future study could focus on detecting any plant species that are unique to burial sites, determine the length of time that soil and vegetation changes persist and recognize any factors that may influence the visibility of graves in arid environments such as larger disturbance areas, fine-textured soils, different subsoils, and the distance from intact vegetation, which has been studied and explored recently but in a different environment [49]. While the complexity of surface anomalies can vary, utilizing the expertise of archaeologists and botanists can aid in developing search techniques for the location of potential burial sites. Additional steps to be considered in any future work to increase the validity of the obtained results include blind testing, whereby the examiner does not have any prior knowledge about the location of the graves when conducting the analysis. This step can be repeated with another observer, neither by revealing the decisions and conclusions of the first examiner nor by knowing what is being verified. Such techniques have been previously used in many other fields in the forensic science community, such as in fingerprint and DNA analyses, to avoid any bias in decision making [50].

5. Conclusions

Throughout the years, detecting clandestine graves has posed a great challenge to forensic investigators. As highlighted, the present study aimed to temporally monitor and evaluate the use of commercially available UAVs coupled with remote sensing technology to detect clandestine graves in an arid environment. More specifically, our research sought to understand the effectiveness of using RGB and multispectral imagery in identifying soil disturbances, exploring differences in surface elevation and evaluating the use of a vegetation index to aid the detection process of clandestine graves in an arid environment. The research addressed the knowledge gap in forensic anthropology concerning detecting clandestine graves in an arid environment using remote sensing techniques. This research provided insight into whether disturbance from the creation of single and mass graves was detectable using multispectral and RGB imagery. This was achieved by analyzing the captured multispectral and RGB images using manual and automated methods. The ability to detect a grave using remote sensing imagery, whether from multispectral or RGB platforms, depends on several factors, including the spatial resolution of the imagery and the size of the grave. Therefore, the success of mass grave detection through remote sensing hinges on carefully considering a variety of issues. In this research, multispectral imagery was a more suitable approach for manually detecting anomalies than the RGB method. Specifically, NIR and Red-Edge wavelengths were found to be the most appropriate for

this type of detection. However, in some instances, the RGB images were more practical to use in the detection process, especially when there was a vegetation cover on the graves compared to their immediate surroundings. Regardless of the type of sensor used, the manual detection method was sustainable for 15 months for both sensors. Also, the automated detection method for both sensors showed encouraging results when using the RX Anomaly Detection tool. It aimed to detect pixels that are different from the rest of the recorded image sequence, reflecting the soil disturbances on the graves.

Depending on the time of the year and the type of image captured, the detection method which was most informative between the three available options varied. Hence, in principle, this research demonstrated that both the RGB and multispectral imagery could be used to identify a disturbance indicative of the creation of a grave, whether empty or full, for a period that is as long as 18 months and possibly more. Here, the presented findings contradict statements by the previously published literature [5,39], who asserts the necessity of having sophisticated hyperspectral sensors in order to locate areas of disturbances. Instead, the results proved that the acquisition of images in some wavelength bands could indeed help in the identification of soil disturbances, which could be related to the location of the graves when conducting a field search for possible burial sites. Multispectral images were also examined to monitor the normalized difference vegetation index (NDVI) from the surface of the graves. In general, the index map of the NDVI showed a minor difference between the graves and their surroundings. It can be said that the use of the NDVI and its index map can be considered a good addition to any existing detection methods used in the area of interest in an arid environment that lacks dense vegetation but might not be as valuable when used by itself.

Using an RGB sensor deployed on a UAV proved its applicability and appropriateness in detecting burial sites in arid environments throughout the research period of 18 months. This conclusion was reached from the results of the anomaly detection method mentioned above. Moreover, the analysis of RGB images using the normalized digital surface model (nDSM) accurately identified burial mounds with a 1 cm difference from ground level.

In summary, there is no simple answer or single technique for the best method to use in clandestine grave detection. It is all constrained by the environment, the size of the grave, the depth of the grave, the number of bodies buried in the grave, the time of the year when conducting the search, the budget dedicated, and the human resources available.

Author Contributions: Conceptualization, F.B. and C.E.; methodology, F.B. and C.E.; software, A.A.; validation, A.A., F.B. and C.E.; formal analysis, A.A.; investigation, A.A.; resources, A.A. and C.E.; data curation, A.A.; writing—original draft preparation, A.A.; writing—review and editing, F.B. and C.E.; visualization, A.A.; supervision, F.B. and C.E.; project administration, C.E.; funding acquisition, A.A. All authors have read and agreed to the published version of the manuscript.

Funding: Abdullah Alawadhi's doctoral research was funded by the Kuwaiti Ministry of Interior.

Data Availability Statement: We understand the importance of presenting detailed data and methods to enable replication, but we will not make raw data publicly available where possible due to their sensitivity.

Acknowledgments: The authors wish to thank the Environment Public Authority of Kuwait for their support in providing the plot of land used in this research.

Conflicts of Interest: The authors declare no conflicts of interest. The funders had no role in the design of the study; in the collection, analyses, or interpretation of data; in the writing of the manuscript; or in the decision to publish the results.

References

1. Eliopoulos, C. Human rights violations in Ukraine: The need for forensic investigations. *Lancet* **2023**, *402*, 772–773. [CrossRef] [PubMed]
2. Blau, S.; Sterenberg, J.; Weeden, P.; Urzedo, F.; Wright, R.; Watson, C. Exploring non-invasive approaches to assist in the detection of clandestine human burials: Developing a way forward. *Forensic Sci. Res.* **2018**, *3*, 304–326. [CrossRef] [PubMed] [PubMed Central]

3. Abate, D.; Sturdy Colls, C.; Moyssi, N.; Karsili, D.; Faka, M.; Anilir, A.; Manolis, S. Optimizing search strategies in mass grave location through the combination of digital technologies. *Forensic Sci. Int.* **2019**, *1*, 95–107. [CrossRef] [PubMed] [PubMed Central]
4. Rocke, B.; Ruffell, A. Detection of Single Burials Using Multispectral Drone Data: Three Case Studies. *Forensic Sci.* **2022**, *2*, 72–87. [CrossRef]
5. Kalacska, M.E. The Application of Remote Sensing for Detecting Mass Graves: An Experimental Animal Case Study from Costa Rica. *J. Forensic Sci.* **2009**, *54*, 159–167. [CrossRef] [PubMed]
6. Fernández-Álvarez, J.-P.; Rubio-Melendi, D.; Martínez-Velasco, A.; Pringle, J.K.; Aguilera, H.-D. Discovery of a mass grave from the Spanish Civil War using Ground Penetrating Radar and forensic archaeology. *Forensic Sci. Int.* **2016**, *267*, e10–e17. [CrossRef]
7. Pollard, T.; Barton, P. The Use of First World War Aerial Photographs by Archaeologists: A Case Study from Fromelles, Northern France. In *Archaeology from Historical Aerial and Satellite Archives*; Hanson, W.S., Oltean, I.A., Eds.; Springer: New York, NY, USA, 2013; pp. 87–103.
8. Parrott, E.; Panter, H.A.; Morrissey, J.; Bezombes, F. A Low Cost Approach to Disturbed Soil Detection Using Low Altitude Digital Imagery from an Unmanned Aerial Vehicle. *Drones* **2019**, *3*, 50. [CrossRef]
9. Butters, O.; Krosch, M.N.; Roberts, M.; MacGregor, D. Application of forward-looking infrared (FLIR) imaging from an unmanned aerial platform in the search for decomposing remains. *J. Forensic Sci.* **2021**, *66*, 347–355. [CrossRef]
10. Silván-Cárdenas, J.L.; Caccavari-Garza, A.; Quinto-Sánchez, M.E.; Madrigal-Gómez, J.M.; Coronado-Juárez, E.; Quiroz-Suarez, D. Assessing optical remote sensing for grave detection. *Forensic Sci. Int.* **2021**, *329*, 111064. [CrossRef]
11. Corcoran, K.A.; Mundorff, A.Z.; White, D.A.; Emch, W.L. A novel application of terrestrial LIDAR to characterize elevation change at human grave surfaces in support of narrowing down possible unmarked grave locations. *Forensic Sci. Int.* **2018**, *289*, 320–328. [CrossRef]
12. Silván-Cárdenas, J.L.; Corona-Romero, N.; Madrigal-Gómez, J.M.; Saavedra-Guerrero, A.; Cortés-Villafranco, T.; Coronado-Juárez, E. On the Detectability of Buried Remains with Hyperspectral Measurements. In *Pattern Recognition*; Lecture Notes in Computer Science; Springer: Cham, Switzerland, 2017; pp. 201–212.
13. Alawadhi, A.; Eliopoulos, C.; Bezombes, F. The detection of clandestine graves in an arid environment using thermal imaging deployed from an unmanned aerial vehicle. *J. Forensic Sci.* **2023**, *68*, 1286–1291. [CrossRef] [PubMed]
14. Almedeij, J. Modeling Rainfall Variability over Urban Areas: A Case Study for Kuwait. *Sci. World* **2012**, *2012*, 980738. [CrossRef]
15. Schuldenrein, J.; Trimble, M.K.; Malin-Boyce, S.; Smith, M. Geoarchaeology, Forensics, and the Prosecution of Saddam Hussein: A Case Study from the Iraq War (2003–2011). *Geoarchaeology* **2017**, *32*, 130–156. [CrossRef]
16. Al-Dossari, F. *Almohima Alkubra: Masirat Albahth Aljinaee [The Grand Mission: The Criminal Investigation]*, 2nd ed.; Al Alfain: Hawally, Kuwait, 2018.
17. Pringle, J.K.; Jervis, J.R.; Hansen, J.D.; Jones, G.M.; Cassidy, N.J.; Cassella, J.P. Geophysical Monitoring of Simulated Clandestine Graves Using Electrical and Ground-Penetrating Radar Methods: 0–3 Years After Burial. *J. Forensic Sci.* **2012**, *57*, 1467–1486. [CrossRef] [PubMed]
18. Matuszewski, S.; Hall, M.J.R.; Moreau, G.; Schoenly, K.G.; Tarone, A.M.; Villet, M.H. Pigs vs. people: The use of pigs as analogues for humans in forensic entomology and taphonomy research. *Int. J. Leg. Med.* **2020**, *134*, 793–810. [CrossRef] [PubMed]
19. DesMarais, A.M. Detection of Cadaveric Remains by Thermal Imaging Cameras. *J. Forensic Identif.* **2014**, *64*, 489–511.
20. Teo, C.; Pawita, A.; Osman, K.; Ghani, A.A.; Hamzah, N.H. Post mortem changes in relation to different types of clothing. *Malays. J. Pathol.* **2013**, *35*, 77–85.
21. Pix4D. *Pix4Dcapture*, 4.13.1 ed.; Pix4D: Lausanne, Switzerland, 2022.
22. Pix4D. *Pix4Dmapper Educational License*, 4.6.4 ed.; Pix4D: Lausanne, Switzerland, 2022.
23. Parrot. *Parrot ANAFI Thermal*; Parrot: Paris, France, 2020.
24. Parrot. *Parrot Bluegrass*; Parrot: Paris, France, 2020.
25. Booysen, R.; Gloaguen, R.; Lorenz, S.; Zimmermann, R.; Nex, P.A.M. Geological Remote Sensing. In *Encyclopedia of Geology*, 2nd ed.; Alderton, D., Elias, S.A., Eds.; Academic Press: Oxford, UK, 2021; pp. 301–314.
26. Assmann, J.J.; Kerby, J.T.; Cunliffe, A.M.; Myers-Smith, I.H. Vegetation monitoring using multispectral sensors—Best practices and lessons learned from high latitudes. *J. Unmanned Veh. Syst.* **2018**, *7*, 54–75. [CrossRef]
27. Aber, J.S.; Marzolff, I.; Ries, J.B. Chapter 3—Photogrammetry. In *Small-Format Aerial Photography*; Aber, J.S., Marzolff, I., Ries, J.B., Eds.; Elsevier: Amsterdam, The Netherlands, 2010; pp. 23–39.
28. *Exelis Visual Information Solutions*, ENVI. 5.6 ed.; L3Harris Geospatial: Boulder, CO, USA, 2020.
29. Reed, I.S.; Yu, X. Adaptive multiple-band CFAR detection of an optical pattern with unknown spectral distribution. *IEEE Trans. Acoust. Speech Signal Process.* **1990**, *38*, 1760–1770. [CrossRef]
30. Chein, I.C.; Shao-Shan, C. Anomaly detection and classification for hyperspectral imagery. *IEEE Trans. Geosci. Remote Sens.* **2002**, *40*, 1314–1325. [CrossRef]
31. ESRI. *ArcGIS Desktop*, 10.8.1.14362 ed.; ESRI: Redlands, CA, USA, 2002.
32. Veerendra, T.M.; Latha, B.M.; Raghudathesh, G.P. Classification of Remotely Sensed Data using ENVI 4.7 Tool. *Int. J. Res. Advent Technol.* **2014**, *2*, 62–66.
33. Sobotkova, A.; Ross, S.A. (Eds.) High-resolution, multi-spectral satellite imagery and extensive archaeological prospection: Case studies from Apulia, Italy and Kazanluk, Bulgaria. In Proceedings of the Third International Conference on Remote Sensing in Archaeology, Tiruchirappalli, India, 17–21 August 2009; Archaeopress: Haryana, India, 2010.

34. Baluja, J.; Diago, M.P.; Balda, P.; Zorer, R.; Meggio, F.; Morales, F.; Tardaguila, J. Assessment of vineyard water status variability by thermal and multispectral imagery using an unmanned aerial vehicle (UAV). *Irrig. Sci.* **2012**, *30*, 511–522. [CrossRef]
35. Casamitjana, M.; Torres-Madroñero, M.C.; Bernal-Riobo, J.; Varga, D. Soil Moisture Analysis by Means of Multispectral Images According to Land Use and Spatial Resolution on Andosols in the Colombian Andes. *Appl. Sci.* **2020**, *10*, 5540. [CrossRef]
36. Korchagina, I.; Goleva, O.; Savchenko, Y.; Bozhikov, T. The use of geographic information systems for forest monitoring. *J. Phys. Conf. Ser.* **2020**, *1515*, 032077. [CrossRef]
37. Barone, P.M.; Matsentidi, D.; Mollard, A.; Kulengowska, N.; Mistry, M. Mapping Decomposition: A Preliminary Study of Non-Destructive Detection of Simulated body Fluids in the Shallow Subsurface. *Forensic Sci.* **2022**, *2*, 620–634. [CrossRef]
38. Dozal, L.; Silván-Cárdenas, J.; Moctezuma, D.; SSiordia, O.; Naredo, E. Evolutionary Approach for Detection of Buried Remains Using Hyperspectral Images. *Photogramm. Eng. Remote Sens.* **2018**, *84*, 435–450. [CrossRef]
39. Leblanc, G.; Kalacska, M.; Soffer, R. Detection of single graves by airborne hyperspectral imaging. *Forensic Sci. Int.* **2014**, *245*, 17–23. [CrossRef] [PubMed]
40. Molina, C.M.; Wisniewski, K.; Heaton, V.; Pringle Jamie, K.; Avila, E.F.; Herrera, L.A.; Guerrero, J.; Saumett, M.; Echeverry, R.; Duarte, M.; et al. Monitoring of simulated clandestine graves of dismembered victims using UAVs, electrical tomography, and GPR over one year to aid investigations of human rights violations in Colombia, South America. *J. Forensic Sci.* **2022**, *67*, 1060–1071. [CrossRef]
41. Murray, B.; Anderson, D.; Wescott, D.; Moorhead, R.; Anderson, M. Survey and Insights into Unmanned Aerial-Vehicle-Based Detection and Documentation of Clandestine Graves and Human Remains. *Hum. Biol.* **2018**, *90*, 45–61. [CrossRef]
42. Rocke, B.; Ruffell, A.; Donnelly, L. Drone aerial imagery for the simulation of a neonate burial based on the geoforensic search strategy (GSS). *J. Forensic Sci.* **2021**, *66*, 1506–1519. [CrossRef]
43. Urbanová, P.; Jurda, M.; Vojtíšek, T.; Krajsa, J. Using drone-mounted cameras for on-site body documentation: 3D mapping and active survey. *Forensic Sci. Int.* **2017**, *281*, 52–62. [CrossRef]
44. Evers, R. The application of low-altitude near-infrared aerial photography for detecting clandestine burials using a UAV and low-cost unmodified digital camera. *Forensic Sci. Int.* **2018**, *289*, 408. [CrossRef]
45. Somma, R.; Cascio, M.; Silvestro, M.; Torre, E. A GIS-based Quantitative Approach for the Search of Clandestine Graves, Italy. *J. Forensic Sci.* **2018**, *63*, 882–898. [CrossRef] [PubMed]
46. Pringle, J.K.; Ruffell, A.; Jervis, J.R.; Donnelly, L.; McKinley, J.; Hansen, J.; Morgan, R.; Pirrie, D.; Harrison, M. The use of geoscience methods for terrestrial forensic searches. *Earth-Sci. Rev.* **2012**, *114*, 108–123. [CrossRef]
47. Sona, G.; Passoni, D.; Pinto, L.; Pagliari, D.; Masseroni, D.; Ortuani, B.; Facchi, A. UAV multispectral survey to map soil and crop for precision farming applications. *Int. Arch. Photogramm. Remote Sens. Spat. Inf. Sci.* **2016**, *XLI-B1*, 1023–1029. [CrossRef]
48. Mann, R.W.; Bass, W.M.; Meadows, L. Time since death and decomposition of the human body: Variables and observations in case and experimental field studies. *J. Forensic Sci.* **1990**, *35*, 103–111. [CrossRef] [PubMed]
49. Watson, C.J.; Ueland, M.; Schotsmans, E.M.J.; Sterenberg, J.; Forbes, S.L.; Blau, S. Detecting grave sites from surface anomalies: A longitudinal study in an Australian woodland. *J. Forensic Sci.* **2021**, *66*, 479–490. [CrossRef]
50. Dror, I.E.; Charlton, D.; Péron, A.E. Contextual information renders experts vulnerable to making erroneous identifications. *Forensic Sci. Int.* **2006**, *156*, 74–78. [CrossRef]